

CHARACTERIZATION OF MULTILAYER PACVD TiN/Ti(B-N)/TiB₂ COATINGS FOR HOT-WORKED TOOL STEELS USING ELECTRON SPECTROSCOPY TECHNIQUES

KARAKTERIZACIJA VEČPLASTNE PACVD TiN/Ti(B-N)/TiB₂ PREVLEKE ZA ORODNA JEKLA ZA DELO V VROČEM S TEHNIKAMI ELEKTRONSKE SPEKTROSKOPIJE

Monika Jenko¹, Djordje Mandrino¹, Matjaž Godec¹, John T. Grant², Vojteh Leskovšek¹

¹Institute of Metals and Technology, Lepi pot 11, Ljubljana, Slovenia

²University of Dayton, 300 College Park, Dayton, OH 45469, USA

monika.jenko@imt.si

Prejem rokopisa – received: 2008-10-13; sprejem za objavo – accepted for publication: 2008-11-18

Multilayer Ti(B-N) layers have been sandwiched between a TiN coating on treated AISI H11 steel and an outermost TiB₂ coating. The films were deposited with plasma-assisted chemical vapour deposition (PACVD) and have been characterized using electron spectroscopy techniques. The thickness of the total coating is 1.6 µm and comprised 21 layers. Earlier studies of such coatings using X-ray diffraction (XRD), energy dispersive spectroscopy (EDS), and wavelength dispersive spectroscopy (WDS) suffer from their relatively large analysis depths. In this work, Field-emission Auger electron spectroscopy (FE-AES) was used to examine the composition of the multilayered films since it has a smaller analysis depth. AES line-scans across cross-sectioned samples and AES depth profiling were used and are shown to be well suited for characterizing these multilayered coatings. These results are compared with combined Field-emission scanning electron microscopy (FE-SEM) and wavelength dispersive spectroscopy (WDS) measurements of the cross-sectioned samples.

Key words: plasma-assisted chemical vapour deposition (PACVD), hard TiN/Ti(B-N) coating, AISI H11 tool steel, Auger electron spectroscopy (AES), Field-emission SEM, wavelength-dispersive spectroscopy (WDS)

Večplastne Ti(B-N) plasti so vrinjene med TiN prevleko jekla AISI H11 in zunano TiB₂ plast. Plasti so bile nanesene po postopku kemijske parne faze ob pomoči plazme (PACVD), raziskali smo jih z različnimi tehnikami osnovanimi na elektronski spektroskopiji. Debelina celotne prevleke iz 21 plasti je 1.6 µm. Prejšnje raziskave tovrstnih prevlek z rentgensko difracijo (XRD), energijsko disperzijsko spektroskopijo (EDS), valovno disperzijsko spektroskopijo (WDS) niso dovolj natančne zaradi relativno velike analizne globine. V članku predstavljamo uporabo Augerjeve elektronske spektroskopije s FEG izvodom elektronov (FE-AES) za raziskavo sestave posameznih plasti v večplastni prevleki. AES linijska analiza preko preseka vzorca in AES globinski profil se je pokazala za zelo primerno za karakterizacijo tovrstnih večplastnih prevlek. Rezultate smo primerjali z meritvami z vrstično elektronsko mikroskopijo s FEG izvodom elektronov (FE-SEM) in valovno disperzijsko spektroskopijo (WDS) na prečno prerezanih vzorcih.

Ključne besede: s plazmo podprt nanos preko kemijske parne faze (PACVD), trde TiN/Ti(B-N) prevleke, AISI H11 orodno jeklo, Augerjeva elektronska spektroskopija (AES) vrstično elektronska mikroskopija s FEG izvodom elektronov (FE-SEM), valovno disperzijska spektroskopija (WDS)

1 INTRODUCTION

Hard thin films, such as Ti(B-N), are well known for providing surfaces with a high hardness, and good corrosion and wear resistance, giving them a wide range of industrial applications^{1–15}. Duplex treatments consisting of plasma nitriding the steel surface first and then using plasma-assisted chemical vapour deposition (PACVD) to deposit the hard coating has proven successful in improving the wear, fatigue and corrosion resistance, as well as the load-carrying capability, of steel substrates^{16–21}. The increasing industrial demand for improved hard coatings with tailored properties for die casting and forging tools requires the development of multi-element and/or multi-phase hard films, as well as a better understanding of their composition.

Most of the published studies of Ti(B-N) film compositions use scanning electron microscopy (SEM), wavelength-dispersive electron-probe microanalysis (EPMA)^{7,8,10,12}, Rutherford backscattering spectroscopy (RBS)⁵, Bragg-Brentano X-ray diffraction (XRD)^{2,4,7,8,9,10,12} and in some cases transmission electron microscopy (TEM)^{4,6}. These techniques suffer from their relatively large analysis depths or lack of depth resolution. In this investigation we have studied PACVD-deposited thin films using Auger electron spectroscopy, which is better suited for Ti(B-N) multilayer characterization. We demonstrate that a combination of techniques such as AES depth profiling and FE-SEM give a better insight into the chemistry and structure of multilayered Ti(B-N) thin films. WDS measurements were made on the same multilayered structure for comparison.

2 EXPERIMENTAL

2.1 Deposition of the multilayered coating

The base material used for the substrate was AISI H11 tool steel with the chemical composition (all in mas %): Fe, 0.39 C, 0.34 Mn, 1.07 Si, 4.93 Cr, 1.26 Mo, 0.35 V, 0.011 Ti, 0.013 P and 0.0004 S. The samples were vacuum heat treated with the same procedure used for forging dies and then plasma nitrided in a Metaplas Ionon HZIW system. The conventional and plasma heating to the working temperature took 3 hours and the nitriding lasted for 24 hours. After nitriding, the samples were polished and sputter cleaned before the multilayered PACVD films were deposited.

The PACVD deposition on the prepared steel was carried out using the standard TiN/Ti(B-N) process developed by Rübig GMBH ²² in a bipolar-pulsed glow discharge at a constant temperature of 530 °C, a pressure of 200 Pa and a bias voltage of -500 V. The deposition process was as follows: 1 hour of TiN, 8 hours of alternating low and high boron-content Ti(B-N) multilayers with the high boron content continuously increasing and, finally, 1 hour of TiB₂. The TiN films were grown using N₂ and TiCl₄, Ar and H₂ gasses, and for the Ti(B-N) layers, BCl₃ was also added to the deposition chamber. The purity of all the gasses used was 99.9%. The coating had a total of 19 alternating Ti(B-N) layers between TiN and TiB₂ resulting in a total layer thickness of 1.6 µm. The multilayer arrangement started with a TiN layer on the steel sample, and finished with a TiB₂ layer as the surface layer. The boron-containing coating was chosen due to its small grain size, typically 5–7 nm, resulting in an increased resistance to plastic deformation and abrasion when compared to TiN ^{16,20,21}.

2.2 AES line scan and AES depth-profile analysis

The AES instrument used was a Thermo Scientific VG Microlab 310-F composed of two ultra-high-vacuum chambers, one for sample insertion and one for the analysis. The electron gun has a thermally assisted Schottky field-emission source that provides a stable electron beam in the range of 0.5 to 25 keV. The electron energy analyzer is of the double-focusing spherical sector type with an electrostatic input lens and can provide an energy resolution of between 0.02% and 2%. The spectrometer has five electron detectors and spectra were acquired with a constant retard ratio (CRR) of 4, which provides an energy resolution that is 0.5% of the pass energy. For the cross-section studies, samples were cross-sectioned using a JEOL Cross Section Polisher, Model SM-09010, and analyzed using an AES linescan at 10 keV beam energy. AES depth profiles of the hard coatings were also measured with a 10 keV electron beam and the sample was sputtered with a 1.2 nA current of Ar ions at 3 keV. The AES data were acquired using Eclipse V2.1 ver07 software and processed using CasaXPS software.

2.3 WDS analysis

A metallographic cross-section of the multilayered TiN/Ti(B-N)/TiB₂ sample was prepared using a classic metallographic procedure with a Gatan PECS 682 ion polisher.

Secondary-electron images and back-scattered electron images were obtained with a JEOL JSM 6500F FE-SEM, with a working distance of 7.1 mm, an accelerating voltage of 8 kV and a beam current of 0.08 nA. By reducing the accelerating voltage to 8 kV, the area of the emitted backscattered electrons was reduced to a level that enabled the separate layers to be imaged. The WDS line scans were obtained in the FE-SEM using the following standards: pure boron for boron analysis, stoichiometric TiN for nitrogen analysis and pure titanium for titanium analysis. The TiN standard was made with thin film deposition, using a Balzers Plasma Sputron; the TiN stoichiometry was confirmed by XRD ¹⁵. The WDS analysis was performed at 5 kV and 10 kV accelerating voltages at currents of 5.0 nA and 9.2 nA, respectively, using an Oxford Instruments INCA WAVE 700.

3 RESULTS AND DISCUSSION

3.1 AES line-scan analysis

Figure 1(a) shows an SEM image of the cross-sectioned, multilayered TiN/Ti(B-N)/TiB₂ hard coating, together with the position where the AES line-scan was made across the sample. **Figure 1(b)** shows the elemental concentrations determined from the AES line scan. The N Auger peak overlaps a Ti Auger peak at 420 eV and the N concentration was calculated by comparing the overlapping peak with the 420 eV Ti Auger peak and applying the following relationships:

$$I_{385} \approx \alpha_{c_N} S_{N\ 385} + \alpha_{c_Ti} S_{Ti\ 385} \quad (1)$$

$$I_{420} \approx \alpha_{c_Ti} S_{Ti\ 420} \quad (2)$$

giving

$$\frac{c_N}{c_{Ti}} \approx \frac{S_{Ti\ 420}}{S_{N\ 385}} \cdot \frac{I_{385}}{I_{420}} - \frac{S_{Ti\ 385}}{S_{N\ 385}} \quad (3)$$

where I_{385} and I_{420} are the peak-to-peak intensities of the overlapping Ti and N peaks at approximately 385 eV and the Ti peak at 420 eV respectively, the S are sensitivity factors for N and Ti peaks at the indicated energies, and the c are the indicated N and Ti concentrations. The combined N and Ti profile were calculated first, then decoupled using the Ti profile from the Ti peak at 420 eV. Note that B decreases while the N increases with distance from the surface, although the undulations of eight of the boron-depleted regions and eight of the boron-rich regions can be seen in the Auger linescan. There also appears to be a relatively flat region in N concentration near the interface with the steel substrate (corresponding to the TiN layer).

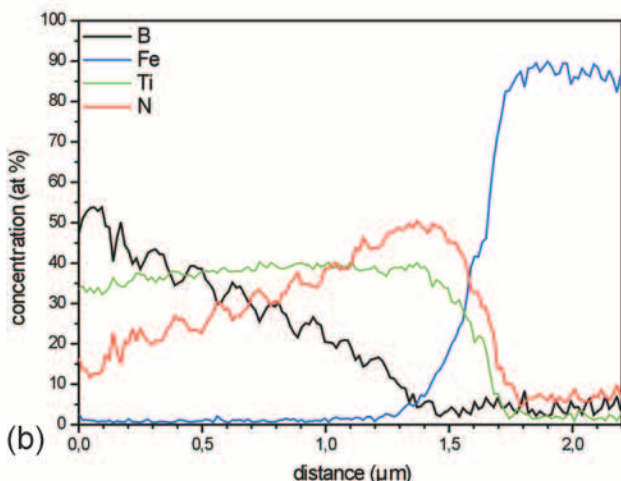
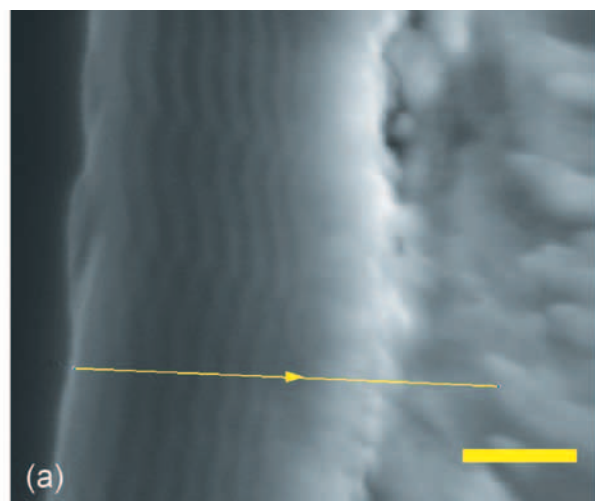


Figure 1: (a) SEM image of the cross sectioned TiN/Ti(B-N)/TiB₂/steel sample showing the region where the AES linescan was made. The scale marker is 600 nm long; (b) concentrations of Ti, N, B and Fe calculated from the AES linescan made along the line shown in part (a)

Slika 1: (a) SEM posnetek preseka vzorca TiN/Ti(B-N)/TiB₂/jeklo, prikazuje področje AES linijske analize. Merilna skala je 600 nm; (b) koncentracija Ti, N, B in Fe izračunana iz AES linijske analize vzdolž linije prikazane v delu (a)

3.2 AES depth profiling

The Auger sputter depth profile is shown in **Figure 2**. The Auger spectra were processed using equation (3), as was done for the Auger linescans. The TiB₂ layer can be seen at the first part of the depth profile. The nine boron-depleted and nine boron-rich regions can be seen in the sputter depth profile, and these are much better resolved than the corresponding regions in the Auger linescan shown in **Figure 1(b)**. Further, not all 18 alternating layers were resolved in the Auger linescan. The close agreement with the boron concentration behaviour in the Auger line scan and the Auger sputter depth profile indicates the absence of preferential sputtering in the depth profile.

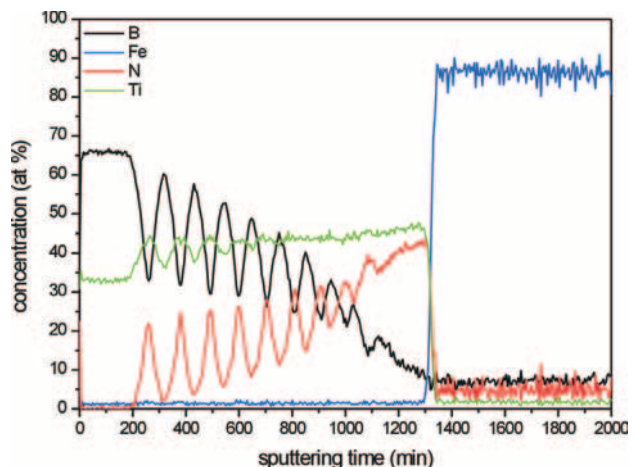


Figure 2: AES sputter depth profile of the TiB₂/Ti(N-B)/TiN multilayered hard coating showing an approximate 15 nm depth resolution

Slika 2: AES globinski profil TiB₂/Ti(N-B)/TiN večplastne trde prevleke prikazuje približno 15 nm globinsko ločljivost

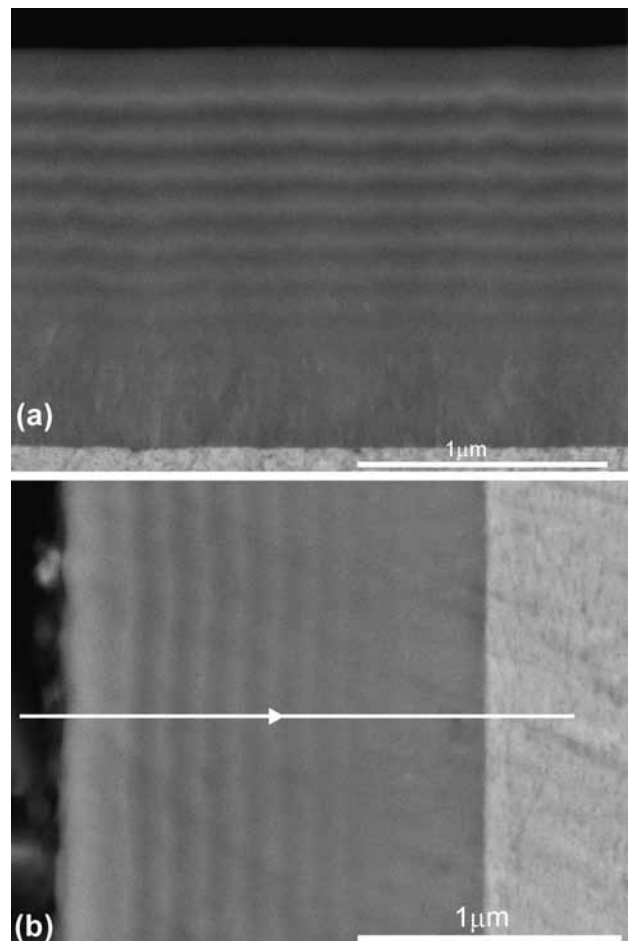


Figure 3: (a) BEI posnetek nanostrukturirane večplastne prevleke vzorca v preseku, (b) BEI posnetek istega vzorca, ki prikazuje področje WDS analize

3.3 WDS analysis

WDS measurements of the TiN/Ti(B-N)/TiB₂ multilayer were made for comparison. **Figure 3(a)** shows a backscattered electron image (BEI) of the nanostructure of a multilayered coated sample in cross-section, allowing to see the whole multilayer structure quite clearly. The first layer of the coating is TiN, and its growth seems to be columnar. Above this layer the multilayer structure of the Ti(B-N) layers are distinguished and finishes with the thicker TiB₂ layer on top. The light-grey regions represent TiN and boron-depleted Ti(B-N) layers, which have a higher average atomic

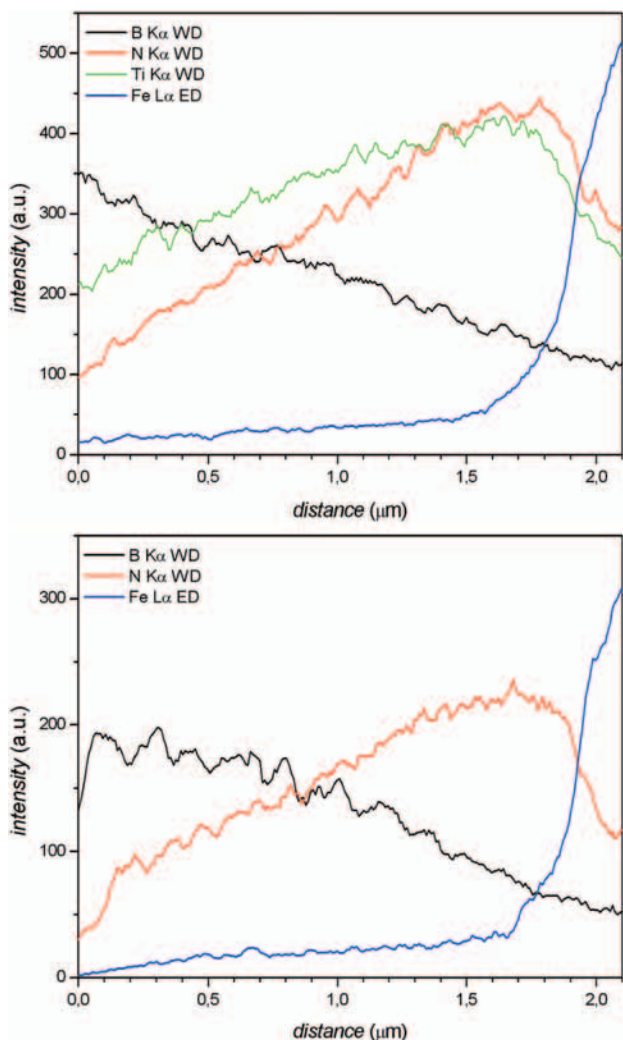


Figure 4: WDS line scans across the multilayer structure, (a) accelerating voltage of the primary electron beam 10 kV, (b) accelerating voltage of the primary beam 5 kV. The multilayered nature of the coating can be best observed from the boron linescan at 5 kV. The Ti K_α linescan is only present at 10 kV since 5 kV is too low for Ti K_α excitation.

Slika 4: WDS linijska analiza preko večplastne strukture, (a) pospeševalna napetost primarnega elektronskega snopa 10 kV, (b) pospeševalna napetost primarnega elektronskega snopa 5 kV. Večplastna struktura je najbolje vidna iz linijske analize bora pri 5 kV. Ti K_α linijska analiza je prisotna samo pri 10 kV, ker je 5 kV premalo za vzbujanje Ti K_α.

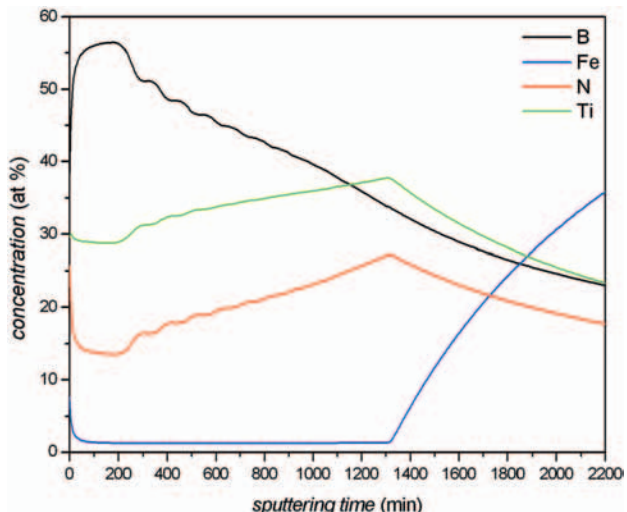


Figure 5: Cumulative depth profiles obtained with calculating the average concentrations between the surface and a given depth from the Auger depth profiles in **Figure 2**. They demonstrate that the average coating composition is heavily dependent on the analysis depth.

Slika 5: Zbirni globinski profil dobljen z izračunom poprečnih koncentracij med površino in dano globino iz Augerjevega globinskega profila na **Sliki 2**. prikazujejo je močno odvisnost poprečne sestave plasti od analizne globine.

number, and the dark-grey regions represent the boron-rich Ti(B-N) and TiB₂ layers, which have a lower average atomic number. The thickness of each layer was estimated to be 65 – 70 nm, except for first TiN and last TiB₂ layers which were each estimated to be approximately 150 nm thick.

Microchemical WDS line analyses were performed to determine the elemental distribution across the multilayer structure. The region where such an analysis was made is shown in **Figure 3(b)**. At a 10 kV accelerating voltage the B, N and Ti K_α x-ray lines are detected and measured. The Fe analysis was performed by EDS using L_a emission. For these conditions, the analyzed volume is of the order of 0.5 μm³. By decreasing the accelerating voltage to 5 kV the analyzed volume is reduced to 0.008 μm³. The line analysis performed at the higher accelerating voltage shows the boron, nitrogen and titanium distribution, **Figure 4(a)**. As expected, the boron concentration is highest at the top layers, and then it decreases to the multilayer-steel interface. The opposite is true for the nitrogen and titanium distributions. Using the lower accelerating voltage of 5 kV, it is possible to see an indication of a multilayer structure with observing the elemental distribution of boron, **Figure 4(b)**. However, the relatively large analysis depth compared to AES severely limited the observation of the layered structure in the coating using WDS. Due to the spatial resolution requirements of this analysis, the low intensity Fe L_a was used as it could be excited at 10 and 5 kV. This prompted the use of EDS instead of WDS for the Fe analysis. However, the inferior signal-to-noise ratio in

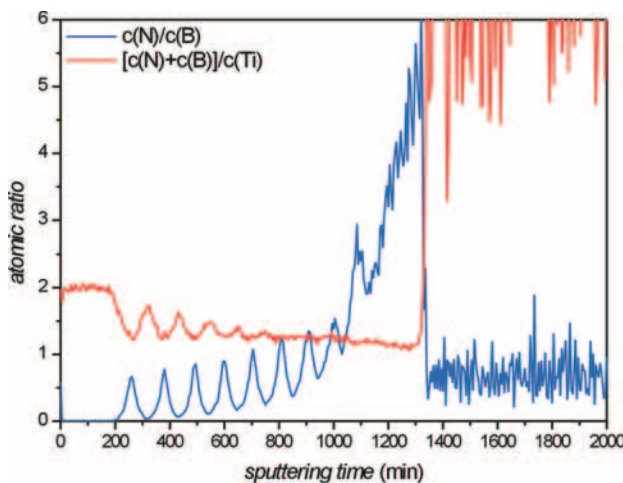


Figure 6: $[c(N)+c(B)]/c(Ti)$ and $c(N)/c(B)$ ratios through the thin film coating, as derived from the AES depth profile shown in **Figure 2**. Close to the surface the stoichiometry corresponds to TiB_2 , although it is close to TiN near the coating-substrate interface.

Slika 6: $[c(N)+c(B)]/c(Ti)$ in $c(N)/c(B)$ razmerja skozi tanko plast prevleke, izpeljan iz AES globinskega profila na **sliki 2**. V bližini površine se stehiometrija ujema z TiB_2 čeprav je blizu TiN na mejni površini prevleka-substrat.

EDS means that some of the noise throughout the layers is mistaken for Fe L_α.

WDS and/or EDS analytical methods are often used to determine the chemical composition of hard coatings e.g.,¹⁵, and even in cases where the thickness of the layer is not large compared to the analysis depth an attempt is made to adjust for it by the proper choice of primary beam energy¹⁶. However, in the case of the multilayer coatings produced in this study, the average composition measured by a non-surface-sensitive technique would look somewhat like that shown in **Figure 5**. The average composition would be extremely dependent on the analysis depth and for small analysis depths even on the surface contamination.

It is also instructive to present depth profiling results in the form of total non-metal/titanium, and nitrogen/boron atomic ratios, as shown in **Figure 6** that shows that close to the surface the composition of the coating corresponds to TiB_2 , while it approaches TiN near the coating-substrate interface. In the intermediate area, a strong variation of the B/N ratio in the Ti(B-N) layers can be clearly observed. All of this agrees with the sample manufacturing procedure, as summarized in section 2.1. The $[c(N)+c(B)]/c(Ti)$ in the Ti(B-N) layers stays mostly below 1.5, which suggests that they may have a cubic structure up until hcp TiB_2 , since TiN_x is cubic for $x < 1.5$ ¹³.

4 CONCLUSION

We have shown that for studies of multilayer TiN/Ti(B-N)/ TiB_2 hard coatings, Auger linescans and

Auger sputter depth profiling are better suited to determine their composition than WDS. WDS suffers from its large analysis volume. Also, Auger sputter depth profiling is superior to Auger linescans for characterizing such films.

Acknowledgement

The authors would like to acknowledge the Ministry of Higher Education, Science and Technology of the Republic of Slovenia and ACRONI d.o.o. for financing the project L2-6093 *Electron spectroscopy of surfaces of nanostructured metallic materials*.

5 REFERENCES

- ¹ W. Gissler, Surf. Coat. Technol. 68/69 (**1994**), 556
- ² T. P. Mollart, M. A. Baker, J. Haupt, A. Steiner, P. Hammer, W. Gissler, Surf. Coat. Technol. 74/75 (**1995**), 491
- ³ T. P. Mollart, P. N. Gibson, M. A. Baker, J. Phys. D: Appl. Phys. 30 (**1997**), 1827
- ⁴ A. Gupper, A. Fernandez, C. Fernandez-Ramos, F. Hoffer, C. Mitterer, P. Warbichler, Monatshefte fur Chemie 133/6 (**2002**), 837
- ⁵ S. M. Aouadi, J. A. Chladek, F. Namavar, N. Finnegan, S. L. Rohde, J. Vac. Sci. Technol. B 20 (**2002**), 1967
- ⁶ M. A. Baker, C. Rebholz, A. Leyland, A. Mathews, Vacuum 67 (**2002**), 471
- ⁷ P. Lossbichler, C. Mitterer, Surf. Coat. Technol. 96 (**1997**), 163
- ⁸ J. Ye, S. Ulrich, K. Sell, H. Leiste, M. Stueber, H. Holleck, Surf. Coat. Technol. 467 (**2004**), 133
- ⁹ P. Karvankova, M. G. J. Veprek-Heijman, O. Zindulka, A. Bergmaier, S. Veprek, Surf. Coat. Technol. 163 (**2003**), 149
- ¹⁰ Y. H. Lu, Y. G. Shen, Z. F. Zhou, K. Y. Li, J. Vac. Sci. Technol. A 24 (**2006**), 340
- ¹¹ C. Mitterer, M. Rauter, P. Rodhammer, S. Veprek, Surf. Coat. Technol. 41 (**1990**), 351
- ¹² P. H. Mayrhofer, C. Mitterer, Surf. Coat. Technol. 133 (**2000**), 134
- ¹³ R. Wiedemann, V. Weihnacht, H. Oettel, Surf. Coat. Technol. 116–119 (**1999**), 302
- ¹⁴ P. H. Mayrhofer, H. Willmann, C. Mitterer, Thin Solid Films, 440 (**2003**), 174
- ¹⁵ P. Panjan, M. Čekada, Zaščita orodij s trdimi PVD prevlekami, Institut Jožef Stefan, Ljubljana 2005 (in Slovene)
- ¹⁶ V. Leskovsek, Some aspects on PACVD, SOHN Inter. Symp. on Advanced Processing of Metals and Mat.: Principles, Technologies and Industrial Practice, San Diego, 27–31 August 2006
- ¹⁷ K.S. Klimek, H. Ahn, I. Seebach, M. Wang, K.T. Rie, Surf. Coat. Technol. 174/175 (**2003**), 1225
- ¹⁸ M. Stoiber, C. Mitterer, T. Schoeberl, E. Badisch, G. Fontalvo, R. Kulmer, J. Vac. Sci. Technol. B 21 (**2003**), 1084
- ¹⁹ M. Stoiber, C. Mitterer, T. Schoeberl, E. Badisch, G. Fontalvo, R. Kulmer, J. Vac. Sci. Technol. B 21 (**2003**), 1084
- ²⁰ P. H. Mayrhofer, M. H. Stoiber, C. Mitterer, Scripta Materialia 53 (**2005**), 241
- ²¹ M. Stoiber, E. Badisch, C. Lugnoir, C. Mitterer, Surf. Coat. Technol. 163 (**2003**), 451
- ²² Micropuls-Plasma-Plastit Rubig GMBH&Co, <http://www.rubig.com>